Degradation-driven protein level oscillation in the yeast *Saccharomyces cerevisiae*

Bahareh Mahrou[1, 2, *], Azady Pirhanov[1], Moluk Hadi Alijanvand[3], Yong Ku Cho[1, 4, *], Yong-Jun Shin[1]

[1] Biomedical Engineering Department, University of Connecticut, Storrs, CT 06269, USA

[2] Electrical Engineering Department, University of Connecticut, Storrs, CT 06069, USA

[3] Department of Epidemiology and Biostatistics, School of Health, Shahrekord University of Medical Sciences, Shahrekord, Iran

[4] Chemical and Biomolecular Engineering Department, University of Connecticut, Storrs, CT 06269, USA

*** Corresponding authors:** Bahareh Mahrou, E-mail: bahareh.mahrou@uconn.edu

Yong Ku Cho, E-mail: cho@uconn.edu

Abstract

Generating robust, predictable perturbations in cellular protein levels will advance our understanding of protein function and enable the control of physiological outcomes in biotechnology applications. Timed periodic changes in protein levels play a critical role in the cell division cycle, cellular stress response, and development. Here we report the generation of robust protein level oscillations by controlling the protein degradation rate in the yeast *Saccharomyces cerevisiae.* Using a photo-sensitive degron and red fluorescent proteins as reporters, we show that under constitutive transcriptional induction, repeated triangular protein level oscillations as fast as 5-10 minute-scale can be generated by modulating the protein degradation rate. Consistent with oscillations generated though transcriptional control, we observed a continuous decrease in the magnitude of oscillations as the input modulation frequency increased, indicating low-pass filtering of input perturbation. By using two red fluorescent proteins with distinct maturation times, we show that the oscillations in protein level is largely unaffected by delays originating from functional protein formation. Our study demonstrates the potential for repeated control of protein levels by controlling the protein degradation rate without altering the transcription rate.

Introduction

Extensive research has led to insights into how the dynamics and complexity of intracellular regulatory networks are organized to maintain a cellular response (Huang and Ingber 2000, Goldberg 2007, Huang and Ingber 2007, Vogel and Marcotte 2012, Ciechanover 2017). One form of regulation is protein turnover, which refers to the continual renewal or replacement of intracellular proteins. The output of this process is the steady-state intracellular protein concentration, maintained dynamically by continuous production and degradation (Hausser, Mayo et al. 2019). The steady-state intracellular protein level shifts in response to extracellular stimuli or pathophysiologic conditions, which cause changes in production or degradation rates (Baracos 2000, Pratt, Petty et al. 2002, Mizushima and Klionsky 2007, Hinkson and Elias 2011, Ciechanover 2017, Kneppers, Langen et al. 2017).

Interestingly, oscillations in the levels of key proteins have been observed in many biological phenomena (Novák and Tyson 2008), including the cell division cycle (Evans, Rosenthal et al. 1983, Glotzer, Murray et al. 1991), circadian rhythm (Kume, Zylka et al. 1999, Reppert and Weaver 2001), cellular stress response (Lahav, Rosenfeld et al. 2004, Geva-Zatorsky, Rosenfeld et al. 2006), and development (Hirata, Yoshiura et al. 2002, Pourquié 2003). In cells, the oscillation of protein levels is achieved by coordinating of many factors, such as transcriptional activities, translation, post-translational control (e.g., phosphorylation), nuclear transport, and targeted protein degradation. A common feature in oscillations is the feedback loop, which can be either positive or negative (Goldbeter 2002, Novák and Tyson 2008). Theoretical models using negative feedback with a time delay can explain a wide range of

protein level oscillations (Lev Bar-Or, Maya et al. 2000, Monk 2003, Tiana, Krishna et al. 2007, Novák and Tyson 2008).

It has been hypothesized that such oscillations enable cells to adapt to periodic changes in the environment (Dunlap 1999), work as a low-pass filter to withstand high-frequency oscillations (Bennett, Pang et al. 2008), repeated repair following DNA damage (Batchelor, Loewer et al. 2009), generate multiple gene expression patterns (Wei, Wu et al. 2006), and potentially integrate multiple cycles of signals before apoptosis (Lahav 2004). A means to elucidate the causal role of protein level oscillations in a key protein would be a robust method to generate timed protein level changes using orthogonal synthetic control decoupled from endogenous signals.

Many versions of synthetic genetic oscillators have been realized through transcriptional control (Novák and Tyson 2008, Purcell, Savery et al. 2010). Although these synthetic design and implementation of oscillators in cells has played a critical role in elucidating the origin and robustness of oscillations (Vilar, Kueh et al. 2002, Purcell, Savery et al. 2010, Woods, Leon et al. 2016), controlling the protein degradation rate has not been explored in synthetic protein-level oscillations. In natural systems, a varying rate of targeted protein degradation has been widely observed in oscillations (Glotzer, Murray et al. 1991, Varshavsky 2008, Batchelor, Loewer et al. 2009). A prominent example is the oscillatory dynamics observed in the tumor suppressor protein p53. Upon DNA damage by γ radiation, the p53 level oscillates without dampening for days (Geva□Zatorsky, Rosenfeld et al. 2006) with the number of pulses increasing as the irradiation dose increases (Lahav, Rosenfeld et al. 2004). The oscillation of p53 is driven by a negative feedback loop between p53 and Mdm2, in which p53 transcriptionally activates Mdm2,

which then binds to p53 and mediates its degradation (Piette, Neel et al. 1997, Lakin and Jackson 1999, Batchelor, Loewer et al. 2009).

Various experimental tools for controlling protein levels have been developed. An extensive list of regulators is available at the transcription level, many of which have been implemented for a wide range of applications (Tigges and Fussenegger 2009, Engstrom and Pfleger 2017, Ding, Zhou et al. 2021). The protein degradation rate can be modulated using degrons, which are short peptide sequences that bind to ubiquitin ligases (Varshavsky 2008, Varshavsky 2019). Harnessing conditional degrons (Natsume and Kanemaki 2017, Luh, Scheib et al. 2020), the protein degradation rate can be controlled by temperature change (Dohmen, Wu et al. 1994, Faden, Ramezani et al. 2016), small molecule binding (Stankunas, Bayle et al. 2003, Banaszynski, Chen et al. 2006, Nishimura, Fukagawa et al. 2009), protease cleavage (Taxis, Stier et al. 2009), or light exposure (Renicke, Schuster et al. 2013, Bonger, Rakhit et al. 2014).

We applied a photo-sensitive degron (psd) (Renicke, Schuster et al. 2013) in *S. cerevisiae* to study the dynamics of protein level oscillations driven by changes in the degradation rate. In this approach, a reporter protein is fused to a photoreceptor protein domain that changes its C-terminal conformation upon blue light exposure. Under blue light, the C-terminally fused degron becomes more accessible, resulting in enhanced protein degradation (**Fig. 1**). Photo-activation provides unique advantages for modulating protein turnover due to the ease of temporal and spatial control of light delivery. In addition, many cell types are not sensitive to light, making them suitable for orthogonal control. We took advantage of the psd developed by Renicke and colleagues to generate frequency-dependent oscillations in protein levels, induced by varying frequency of light inputs to modulate the protein degradation.

Using this system, we observed that robust protein level oscillations can be generated by modulating only the protein degradation rate under constitutive induction. The frequency of oscillation followed that of the input light illumination frequency down to the 5-10 minute scale. We also compared the degradation-driven oscillations of two red fluorescent proteins with distinct maturation times to assess how delays originating during functional protein formation affect protein level oscillation. By quantitatively comparing the oscillation amplitude and phase shift as a function of input frequency, we demonstrate that the oscillations at the protein level are largely unaffected by production delays. Overall, we find that protein level oscillations can be robustly generated simply by modulating the protein degradation rate.

Figure 1.

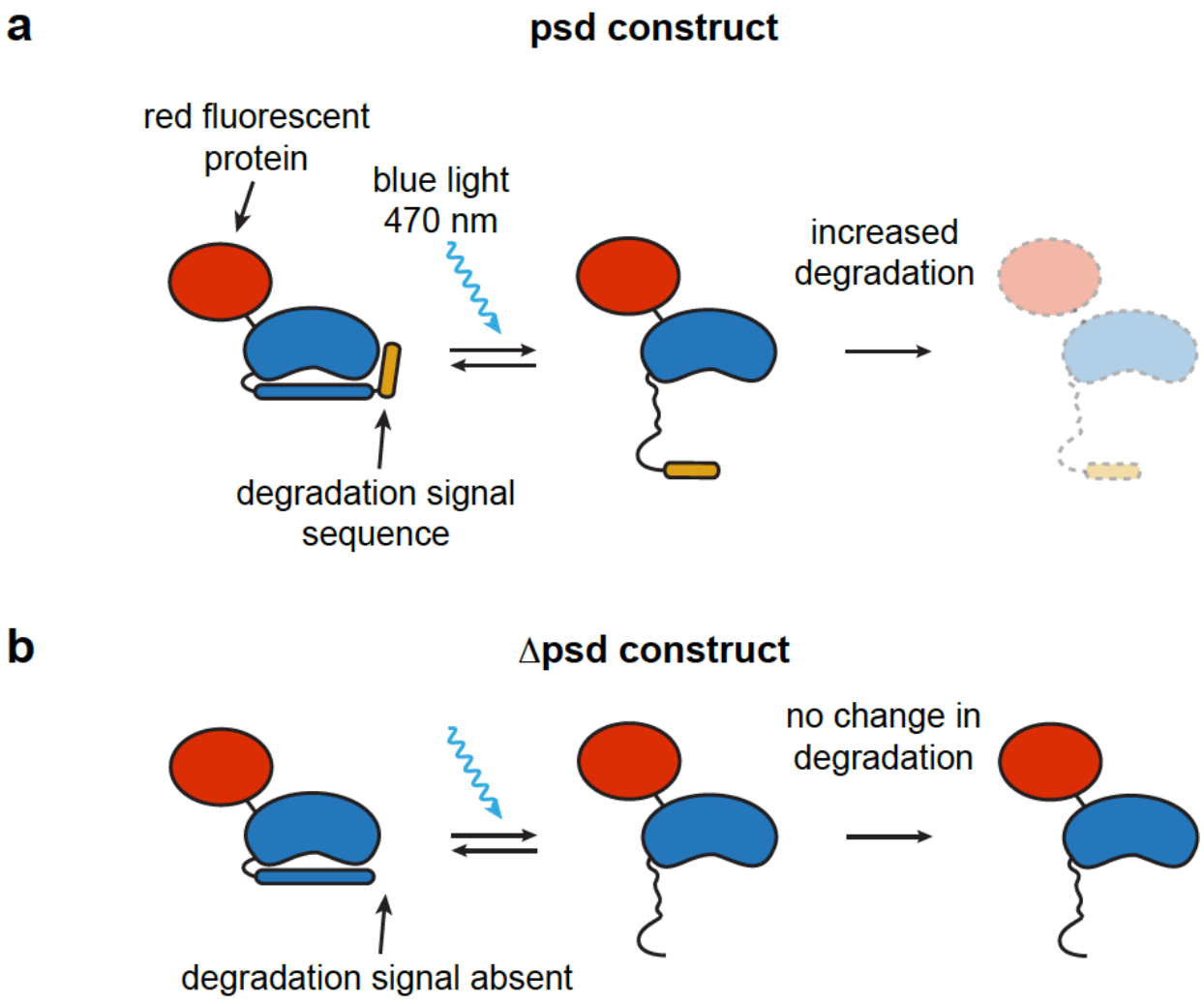

Figure 1. Schematic of photo-sensitive degron (psd) constructs used in this study. In the psd construct (**a**), a protein degradation signal sequence derived from the ornithine decarboxylase is fused to the blue-light sensing light-oxygen-voltage (LOV) domain from *Arabidopsis thaliana*. Upon blue light activation, the degradation signal accessibility increases, resulting in faster protein degradation. The Δpsd construct (**b**), contains all components of psd except the degradation signal sequence.

Results and Discussion

Degradation-driven protein level oscillations in the yeast *S. cerevisiae*

The psd module (**Fig. 1**) comprises the light oxygen voltage 2 domain from *Arabidopsis thaliana* (*At*LOV2), fused with a derivative of the carboxyl-terminal degron of murine ornithine decarboxylase (ODC), enabling the control of the ubiquitin-independent proteasomal degradation rate on blue light illumination (Renicke, Schuster et al. 2013). While *At*LOV2 is sensitive and responsive to blue light, the ODC degradation signal is responsible for increased protein degradation (**Fig. 1**). To observe the effect of modulating the protein degradation rate on protein turnover, we applied pulses of blue light and monitored the fluorescence emission from the red fluorescent protein tagRFP fused to psd (**Fig. 1a**). To validate protein degradation due to the ODC degradation signal, we generated a control construct lacking the signal sequence, termed Δpsd (**Fig. 1b**). The expression of these constructs in yeast *S. cerevisiae* was continuously driven using the $GAL_{1\text{-}10}$ promoter under galactose. To validate continuous expression, we measured the *tagRFP* transcript level by extracting the mRNA from yeast cells and performing a quantitative polymerase chain reaction (qPCR) of the transcript (**Fig. 2a,** see **Supp. Fig. 1** and **Supp. Table 1** for RNA quality control and primers used). Previous studies indicated that prolonged exposure (> 10 hr) of extremely high intensity light (> 10-fold higher intensity used in this study) causes oxidative stress in yeast (Bodvard, Wrangborg et al. 2011, Robertson, Davis et al. 2013). To assess any potential effect of illumination on gene expression, we illuminated the cells with the maximum blue light intensity used in this study (light power density of 0.027 mW/mm^2 [106.02 $\mu mol/m^2s$]) and the longest duration ($1/f$ = 100 min where f indicates the illumination frequency). The mRNA was extracted from cells at the start of the experiment and at the end of each illumination cycle (see inset in **Fig. 2a**). Two primer sets binding to different regions of *tagRFP*

were used for amplification, along with primers for two previously validated housekeeping genes, *TFC1* and *UBC6* (Teste, Duquenne et al. 2009), as a reference. The expression of *tagRFP* remained unchanged for 200 min, and a significant increase was detected between 200 and 300 min (**Fig. 2a**, p = 0.014 and 0.023, student's t-test comparing ΔCt at 200 min. to that at 300 min. for the two *tagRFP* primer sets, respectively [n = 3 independent culture preparations]). This result indicates that the $GAL_{1\text{-}10}$ promoter allows continuous expression of the tagRFP constructs, unhindered by light illumination.

Figure 2.

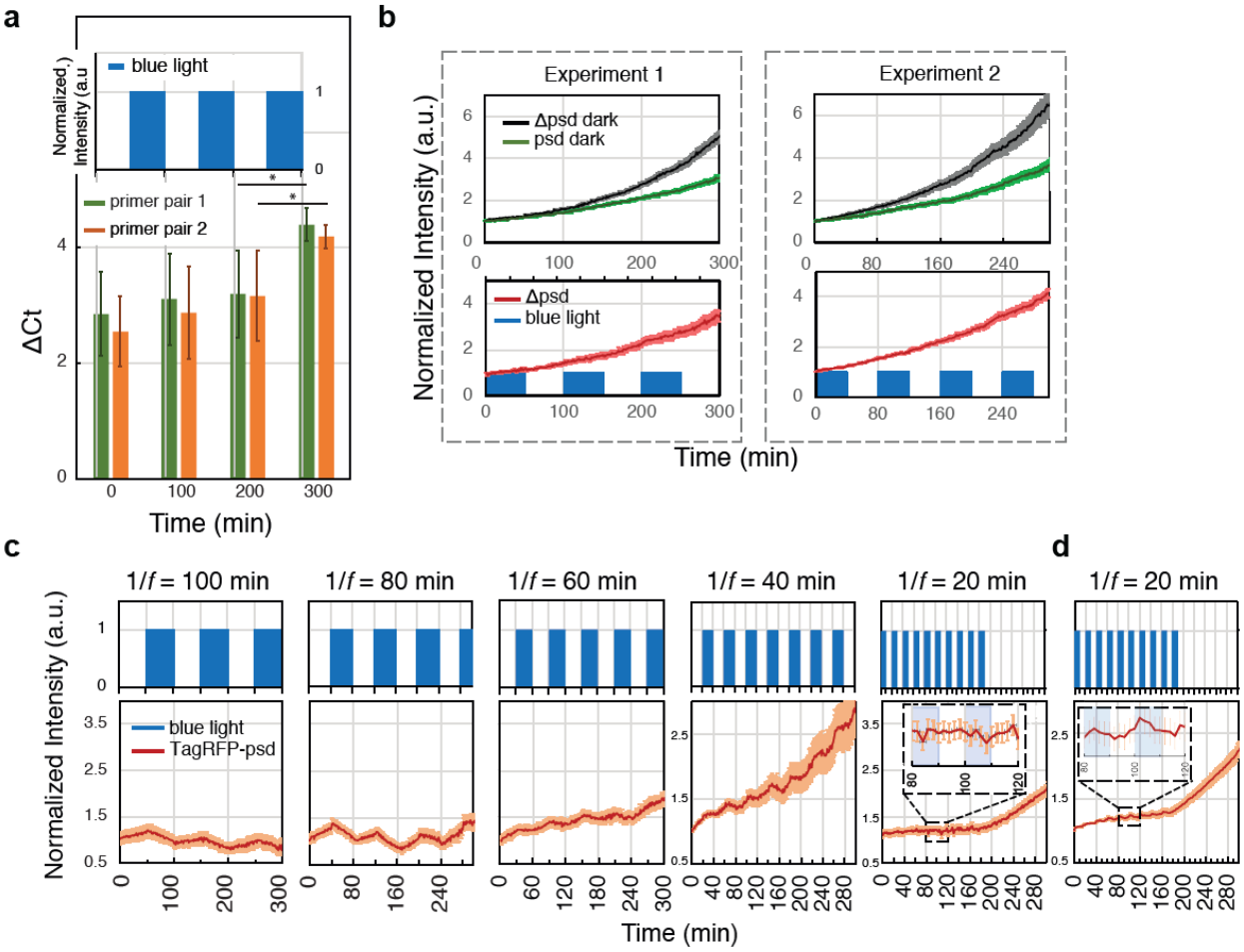

Figure 2. Experimental validation and observation of degradation-driven protein level oscillations in yeast expressing tagRFP fused to psd or Δpsd. (**a**) qPCR analysis of *tagRFP* transcripts during blue light illumination (inset indicates illumination timepoints). Two sets of primers (primer sets 1 and 2) binding to different regions of *tagRFP* were used, and previously validated housekeeping genes *TFC1* and *UBC6* were used as references. The ΔCt values were calculated by subtracting the Ct of *tagRFP* from the average of the Ct of the two reference genes. *: $p < 0.05$, student's t-test comparing ΔCt at 200 min. to that at 300 min. Error bars indicate standard deviation from n = 3 independent culture preparations. (**b**) Normalized fluorescence levels of tagRFP-psd and tagRFP-Δpsd in the dark (top panels); tagRFP-Δpsd illuminated with blue light cycles (bottom panels). Solid lines indicate the mean fluorescence intensities and lighter lines indicate the standard deviation from n = 10 to 15 microcolonies. (**c**) Fluorescence of tagRFP-psd under varying frequencies of blue light illumination. *f* denotes the temporal frequency and 1/*f* indicates the cycle period. Solid lines indicate the mean fluorescence intensities and lighter lines indicate standard deviation from n = 10 to 15 microcolonies. (**d**) Experiment for 1/*f* = 20 min. was repeated with 25 microcolonies. The same intensity of blue light (power density of 0.027 mW/mm^2 [106.02 μmol/m^{2}s]) was used in all panels. In panels (b) and (c), data for each illumination frequency were obtained in separate experiments using independent cell cultures and each microcolony contained 4 to 8 cells at the beginning of experiment.

Since the cell cycle of *S. cerevisiae* is of the order of 100 min (Herskowitz 1988), we observed cell division during the repeated illumination cycles (**Supp. Fig. 2**). The proteins in each cell are divided into daughter cells, resulting in protein dilution. One approach to quantify all the proteins throughout cell division is to sum the fluorescence intensity from a microcolony of cells originating from mother cells (Talia, Skotheim et al. 2007). Consistent with other studies, we found that summing the fluorescence intensity of a microcolony of cells resulted in a continuous increase (red line in **Supp. Fig. 2**), while the fluorescence intensity divided by the area of cells fluctuated as the cells divided (blue line in **Supp. Fig. 2**). To capture the change in protein level decoupled from cell division, we used the sum of the fluorescence intensities of a microcolony of cells as a measure of protein levels throughout this study.

We then tested the effect of pulses of blue light on yeast cells expressing tagRFP-psd or tagRFP-Δpsd. In the absence of blue light, the normalized fluorescence level of tagRFP-psd and tagRFP-Δpsd (see **Materials and Methods** section for calculation) showed a continuous increase over 300 min. (**Fig. 2b**). The fluorescence level of tagRFP-Δpsd was generally higher than that of tagRFP-psd (**Fig. 2b**), probably because the LOV domain conformation was in equilibrium between active and inactive states even in the dark (Strickland, Yao et al. 2010), resulting in slight background degradation even without blue illumination. As anticipated, the level of tagRFP-Δpsd was unresponsive to two distinct illumination frequencies (**Fig. 2b**, f = 1/100 min and f = 1/80 min, respectively in experiments 1 and 2). Conversely, the fluorescence level of tagRFP-psd showed distinct oscillations with varying frequencies of blue light (**Fig. 2c**). We repeated the experiment five times, each at a distinct illumination frequency (**Fig. 2c**). Protein level oscillation was clearly visible up to an illumination frequency of $1/f$ = 40 min, but not at the highest illumination frequency tested ($1/f$ = 20 min) (**Fig. 2c**). When the experiment for

$1/f$ = 20 min was repeated with a larger number of microcolonies, the oscillation was discernable albeit markedly reduced (**Fig. 2d**). Based on these findings, we conclude that the output oscillations observed in the experiment were the result of periodic light-induced alterations in the protein degradation rate mediated by the psd.

Degradation-driven oscillations in a faster maturing fluorescent protein.

Fluorescent proteins contain a chromophore formed through autocatalytic maturation (Wachter 2007, Craggs 2009, Subach and Verkhusha 2012). The fluorescence is only detected after maturation, effectively causing a decrease in the apparent protein production rate. Although not tested, a shift in protein maturation time is expected to impact the low-pass filtering behavior when the transcription rate is modulated as in Bennett *et al.*'s work (Bennett, Pang et al. 2008). Conversely, when the protein degradation rate is modulated, as in our experiments, a shift in protein maturation time should not affect the oscillation behavior. Validating this would indicate that by modulating the protein degradation rate, consistent protein level oscillations can be generated for proteins with distinct production rates.

To test this, we replaced tagRFP in tagRFP-psd with the fluorescent protein mCherry (mCherry-psd), which has a significantly shorter maturation time compared to that of tagRFP (maturation half-time of ~40 min for mCherry vs. ~100 min for tagRFP (Merzlyak, Goedhart et al. 2007)). We then repeated the experiment shown in **Fig. 2c** using mCherry-psd and monitored the mCherry fluorescence in microcolony numbers similar to that in **Fig. 2d** (25 to 30 microcolonies of 4 to 8 cells at the beginning of the experiment). Clear oscillations in mCherry fluorescence were visible, down to an illumination frequency of $1/f$ = 20 min (**Fig. 3a**). We also conducted more experiments with higher input frequencies ($1/f$ = 10 min and $1/f$ = 5 min) and detected small but distinguishable oscillations (**Fig. 3b** and see **Supp. Fig. 4** for extended

experiments). We observed consistent decrease in the amplitudes of output oscillations on increasing the frequency of degradation oscillation, characteristic of a low-pass filtering behavior.

Figure 3.

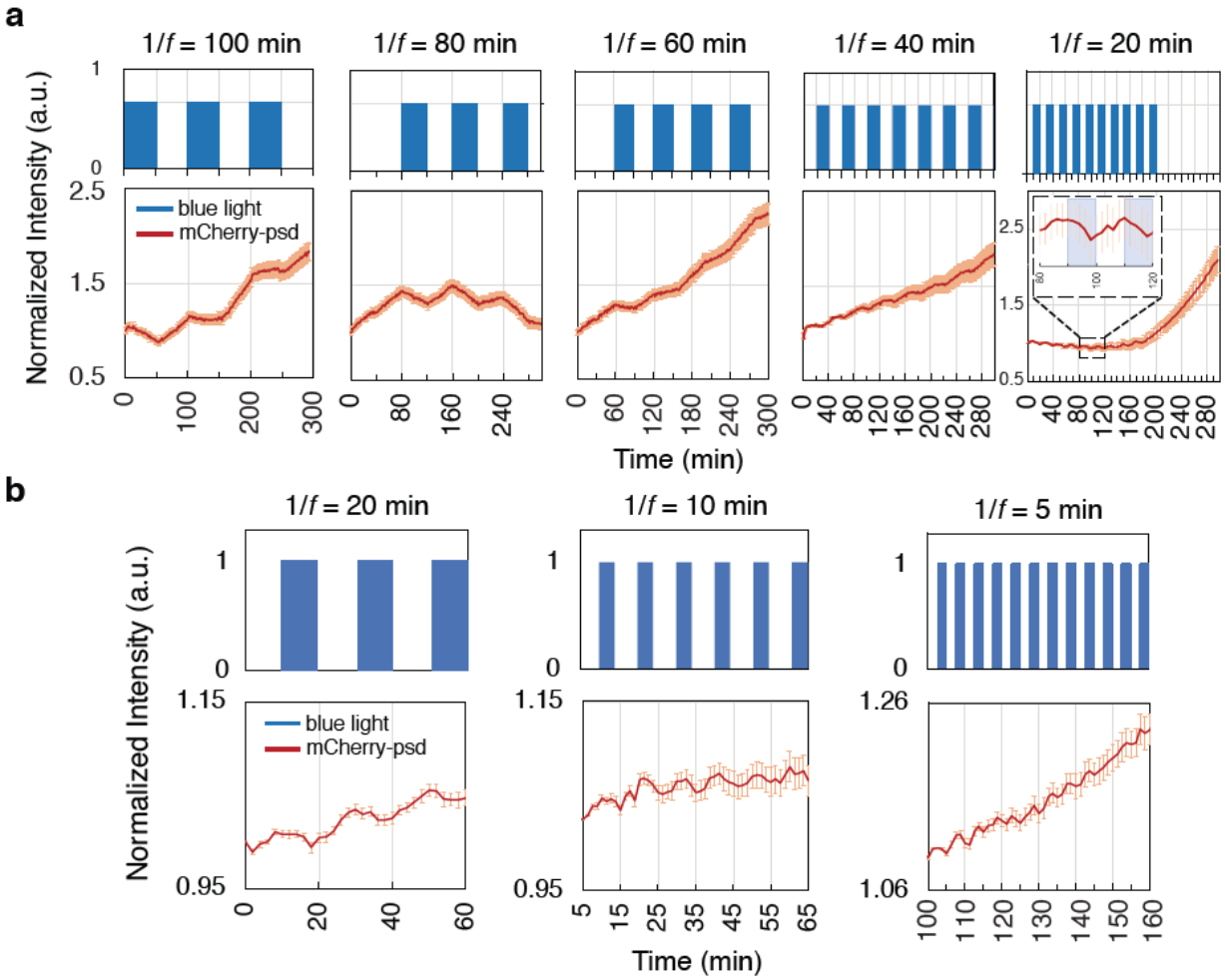

Figure 3. Experimental observation of degradation-driven protein level oscillations in yeast expressing mCherry fused to psd. (**a**) Fluorescence of mCherry-psd under varying frequencies of blue light illumination. (**b**) Fluorescence of mCherry-psd under higher frequency illumination. For frequency $1/f$ = 20 min., the experiment in panel (a) was repeated. For all panels, solid lines indicate the mean fluorescence intensities and lighter lines indicate the standard deviation from n = 25 to 30 microcolonies. The blue light intensity was 0.027 mW/mm^2 (106.02 μmol/m^{2}s)) for all panels. Each microcolony contained 4 to 8 cells at the beginning of experiment.

System identification and frequency-domain analysis.

The reduction in oscillations in protein levels at higher input illumination frequencies is characteristic of low-pass filtering (Antoniou 2016), and indicates that the input perturbation driving protein degradation was filtered out at these higher frequencies. To analyze the low-pass behavior of the degradation driven protein turnover, we determined the time delay between the input blue light illumination frequency and output protein fluorescence intensity using cross-correlation. We calculated the cross-correlation (see **Supplementary Information** for calculation) for experiments using tagRFP-psd and mCherry-psd for frequencies $1/f$ = 40, 60, 80, and 100 (**Fig. 4**). Since the protein level decreased on illumination, a minimum occurred in the cross-correlation (**Fig. 4**, indicated by arrows). Based on the minimum value for each experiment, the time delay between the input and output signals ranged from 1 to 15 min (see **Supplementary Information** for calculation). For both tagRFP-psd and mCherry-psd, we found that the time at which minima occurred shortened as the input frequency oscillations increased, characteristic of a low-pass filtering system.

Figure 4.

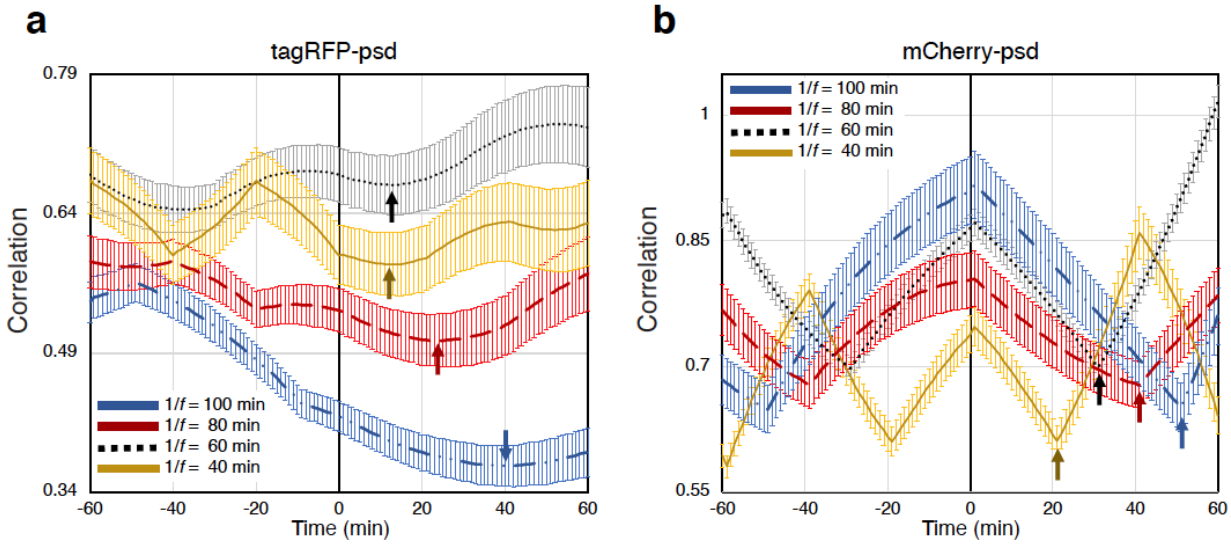

Figure 4. Cross-correlation between input blue light illumination and protein fluorescence intensity. The curves are cross-correlations resulted from experiments with varying input frequencies for tagRFP-psd (**a**) and mCherry-psd (**b**). The arrows show the minimum (after time 0) of each curve. Note that the

minima do not directly indicate the time delay but allow the calculation of the time delay as shown in the Supplementary Information.

To quantitatively assess the low-pass filtering, we constructed a mathematical model for degradation-driven protein turnover using the difference equation approach we previously described (Shin 2016). The model equation can be expressed as

$$y(n) = p_y y(n-1) + p_{pro} u_{pro}(n-1) + p_{deg} u_{deg}(n-1) \quad (1)$$

where n is the discrete-time index, y(n) is the normalized fluorescence intensity at time n, $u_{pro}(n)$ is the normalized amount of galactose (transcription inducer) at time n, and $u_{deg}(n)$ is the normalized intensity of blue light (degradation rate controller) at time n. Parameters p_y, p_{pro}, and p_{deg} indicate endogenous degradation, production, and light-induced degradation, respectively. These parameters can be adaptively estimated from the experimental data using the normalized least mean square (NLMS) algorithm, one of commonly used adaptive system identification algorithm (Ljung 1998, Sayed 2011). Assuming constant protein production, as indicated by relatively consistent transcription (**Fig. 2a**), Equation 1 can be simplified by approximating $u_{pro}(n)$ to 1:

$$y(n) = p_y y(n-1) + p_{pro} + p_{deg} u_{deg}(n-1) \quad (2)$$

Equation 2 represents a multiple-input single-output (MISO) system that can be transformed into the frequency domain using the z–transform.

$$Y(z) = \frac{p_{deg}}{z-p_y} U_{deg}(z) + \frac{p_{pro} z^2}{(z-1)(z-p_y)} \quad (3)$$

Equation 3 illustrates the relationship between the single output Y(z) and two independent inputs (blue light intensity, $U_{deg}(z)$, and the normalized galactose concentration which is assumed to be constant at 1). The equation can be reexpressed in matrix form:

$$Y(z) = \begin{bmatrix} \frac{p_{deg}}{z-p_y} & \frac{p_{pro}z^2}{(z-1)(z-p_y)} \end{bmatrix} \begin{bmatrix} U_{deg}(z) \\ 1 \end{bmatrix} = [H_1(z) \quad H_2(z)] \begin{bmatrix} U(z) \\ 1 \end{bmatrix} \tag{4}$$

$$H_1(z) = \frac{p_{deg}}{z-p_y} \tag{5}$$

$$H_2(z) = \frac{p_{pro}z^2}{(z-1)(z-p_y)} \tag{6}$$

Here, $H_1(z)$ shows the relationship between the output Y(z) (protein fluorescence intensity) and input $U_{deg}(z)$ (blue light intensity). The unknown parameter values p_y and p_{deg} in $H_1(z)$ were estimated using the NLMS adaptive system identification algorithm (See **Supplementary Information** and **Supp. Fig. 5**). The Bode plot in **Fig. 5** (indicated as "Model") shows the amplitude and phase shift response of $H_1(z)$, calculated based on the mean and standard deviation of estimated parameter values acquired from each experiment (See **Supplementary Information**). The amplitude responses demonstrate low-pass filtering, indicated by a steady decrease in the oscillation amplitude as the input blue light illumination frequency increases (**Fig. 5a**). We performed a statistical comparison of the experimental results (tagRFP-psd vs. mCherry-psd) and experiments to the model (tagRFP-psd vs. model, mCherry-psd vs. model). The summary of statistical comparisons in **Table 1** shows that the model effectively captured the amplitude and phase shift responses well. Regarding the amplitude response, no significant difference was found when comparing the model vs. tagRFP-psd or the model vs. mCherry-psd (**Fig. 5a** and **Table 1**). When comparing the phase shift response of the model vs. tagRFP-psd, a significant difference was found for $1/f$ = 100 min, $1/f$ = 80 min, and $1/f$ = 60 min but not at other

frequencies (**Fig. 5b** and **Table 1**). The phase shift response of the model vs. mCherry-psd was significantly different only at illumination frequency of $1/f$ = 100 min (**Fig. 5b** and **Table 1**). When comparing tagRFP-psd vs. mCherry-psd, mCherry-psd showed significantly smaller amplitude responses at frequencies $1/f$ = 80 min, $1/f$ = 60 min, and $1/f$ = 40 min (**Fig. 5a** and **Table 1**), and significantly smaller phase shift at $1/f$ = 60 min, but no difference was found at other frequencies (**Fig. 5b** and **Table 1**). These results show that both tagRFP-psd and mCherry-psd showed low-pass filtering with similar time delays and confirm that the difference in maturation time between tagRFP and mCherry does not cause a significant change in oscillatory behavior at a wide range of frequencies. Comparing the Bode plot of our experiments with the previous study using transcriptional control (Bennett, Pang et al. 2008), we found that the same amplitude of oscillations (e.g., an amplitude of around 0.3 which is equivalent to -10.5 dB) was achieved at approximately 3-fold higher frequencies (0.06 rad/min) under degradation-driven control (achieved at frequency of 0.02 rad/min), indicating that larger oscillations can be generated at higher frequencies. Taken together, these results demonstrate that degradation driven control is a robust approach to generating protein level oscillations on minute timescales.

Although we demonstrated this capability in the yeast *S. cerevisiae*, we anticipate the approach will be applicable to generating protein level oscillations in many other cell types, considering the ODC degron is functional in vertebrates (Murakami, Matsufuji et al. 1992, Takeuchi, Chen et al. 2008) and non-vertebrate species (DeScenzo and Minocha 1993, Hoyt, Zhang et al. 2003). Light-sensitive degradation using the psd has been successfully demonstrated in cell types including human, and other mammalian cells (Sun, Zhang et al. 2017, Baaske, Gonschorek et al. 2018). Moreover, light-activation is highly suitable for feedback control since the intensity, frequency, and location of illumination can be instantly modulated. Since we

demonstrated that controlling the degradation rate is sufficient to drive protein levels under constant transcription, we anticipate this approach to allow generating protein oscillations decoupled from transcriptional signals. This approach may help elucidate the role of oscillations observed in proteins with complex regulatory inputs such as the p53 (Lahav 2004, Porter, Fisher et al. 2016, Harton, Koh et al. 2019) on its downstream gene activation.

Figure 5.

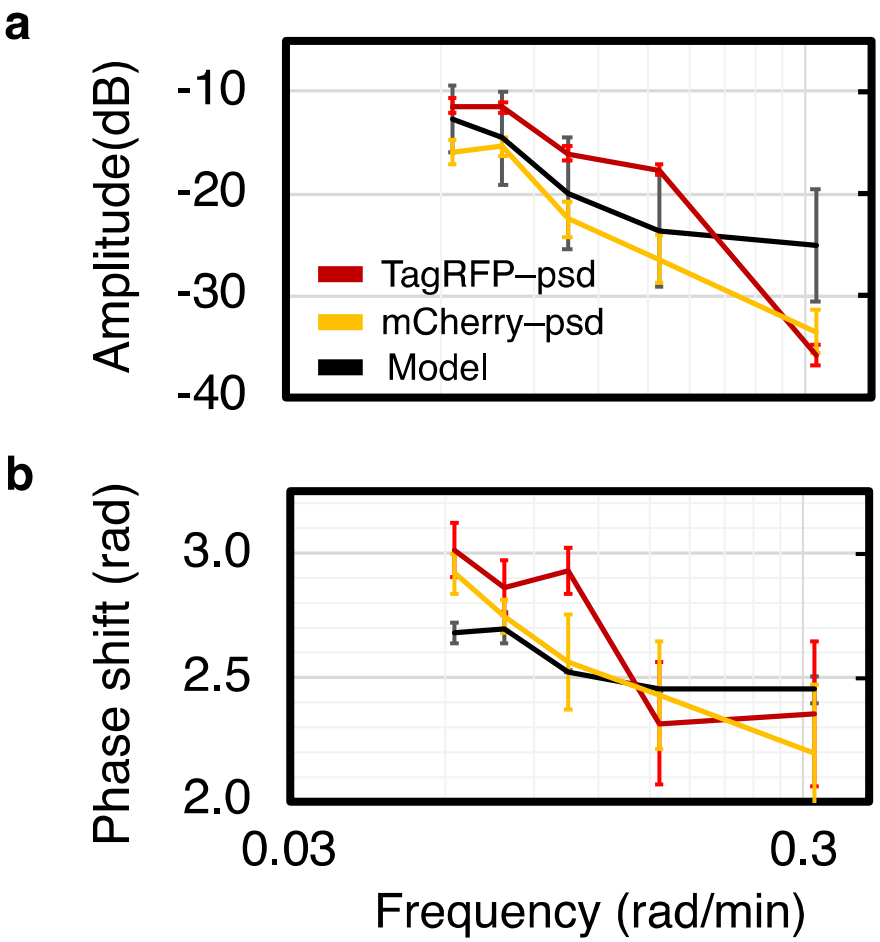

Figure 5. Model and experimental comparison of low-pass filtering using Bode plots. (**a**) Amplitude response and (**b**) phase shift response from tagRFP-psd, mCherry-psd, and model calculations as a function of the input frequency. Data points indicate the median and error bars indicate the interquartile range (IQR) from 10 microcolonies. Statistical analysis of the results is provided in Table 1.

Table 1.

Group \ Set	f = 2π/100 (1/f = 100 min)		f = 2π/80 (1/f = 80 min)		f = 2π/60 (1/f = 60 min)		f = 2π/40 (1/f = 40 min)		f = 2π/20 (1/f = 20 min)	
	Amplitude	Phase shift	Amplitude	Phase shift	Amplitude	Phase shift	Amplitude	Phase shift	Amplitude	Phase shift
	Median (interquartile range, IQR)									
Model	-12.691 (6.657)	2.681 (0.081)	-14.579 (9.136)	2.701 (0.127)	-20.007 (10.840)	2.527 (0.008)	-23.572 (11.131)	2.454 (0.002)	-25.096 (4.847)	2.454 (11.196)
tagRFP-psd	-11.373 (1.498)	3.016 (0.220)	-11.537 (1.149)	2.867 (0.216)	-16.055 (1.421)	2.932 (0.183)	-17.657 (1.205)	2.317 (0.491)	-35.654 (2.146)	2.356 (0.589)
mCherry-psd	-15.918 (2.385)	2.922 (0.157)	-15.391 (1.972)	2.749 (0.137)	-22.518 (3.352)	2.566 (0.380)	-26.478 (4.660)	2.435 (0.432)	-34.437 (4.413)	2.199 (0.550)
P-value Model vs tagRFP-psd	0.438533	0.0001	0.079751	0.0017	0.063264	0.0066	0.079751	0.7342	0.330421	0.9231
P-value Model vs mCherry-psd	0.620585	0.0019	0.918717	0.1961	0.979021	0.9541	0.918717	0.9851	0.620585	0.4881
P-value tagRFP-psd vs mCherry-psd	0.0842	0.7265	0.0094	0.1961	0.0049	0.0161	0.0069	0.8287	0.5037	0.7265

Gray highlighted cells in each column indicate pairs with a significant difference as assessed using the Nemenyi test for multiple pairwise comparisons between the groups, P-value < 0.05

Conclusions

Here we demonstrated robust generation of controlled protein level oscillations in the yeast *S. cerevisiae* using a photo-sensitive degron. We found that by monitoring the total fluorescence of microcolonies of cells, protein oscillations on minute timescales could be reproducibly generated. Using two red fluorescent proteins with distinct maturation times, we showed that the apparent delay in functional protein formation does not change the protein level oscillation generated by modulating the protein degradation rate. The results show that controlling protein degradation rates under constant transcription as a means of modulating protein levels demonstrates a clear pathway for feedback control of protein levels on minute timescales.

Materials and Methods

Cloning and expression of a photo-sensitive degron in yeast

The photo-sensitive degron (psd) module used in this study has been previously described by Renicke and colleagues (Renicke, Schuster et al. 2013). A red fluorescent reporter protein (tagRFP) was fused to the N-terminus of *At*LOV2. The tagRFP-psd construct was cloned into the pRS316 plasmid (Huang and Shusta 2005) (a gift from Dr. Eric Shusta) using restriction enzymes NotI and BsrGI (New England Biolabs) under the galactose inducible $GAL_{1\text{-}10}$ promoter. A psd without the ODC degron (Δpsd) was generated using polymerase chain reaction and cloned using the same restriction sites. The resulting plasmids were named pRS316-tagRFP-psd and pRS316-tagRFP-Δpsd respectively. The plasmids were transformed into the yeast *Saccharomyces cerevisiae* strain BJ5464 (BJα, α *ura3-52 trp1 leu2Δ1 his3Δ200 pep4:: HIS3*

prb1Δ1.6R can1 GAL) cells, using a commercially available kit (Zymo Research). Transformed cells were grown in SD-CAA medium (0.1 M sodium phosphate, pH 6.0, 6.7 g/L yeast nitrogen base, 5.0 g/L casamino acids, 20.0 g/L glucose), supplemented with tryptophan (0.04 g/L) at 30 ^{o}C on an orbital shaker (250 rpm).

qPCR gene expression analysis

Briefly, cells containing pRS316-tagRFP-Δpsd plasmid were grown in SD-CAA medium supplemented with tryptophan (0.04 g/L) at 30 ^{o}C on an orbital shaker (250 rpm) overnight. Yeast cells grown overnight were diluted to an OD_{600} of 1, and the medium was replaced with the induction medium, SG-CAA (0.1 M sodium phosphate, pH 6.0, 6.7 g/L yeast nitrogen base, 5.0 g/L casamino acids, 20.0 g/L galactose) supplemented with tryptophan (0.04 g/L) and incubated at 16 ^{o}C on an orbital shaker (250 rpm) for 20 hr. The cells were then diluted 5-fold in SG-CAA (supplemented with tryptophan) and grown at 30 ^{o}C on an orbital shaker (250 rpm) for period of 400 min with blue light illumination with period of $1/f$ = 100 min. Cells (10 mL of culture) were collected at the end of each 100 min illumination cycle (blue light power density of 0.027 mW/mm^2 (106.02 μmol/m^{2}s)), and stored at 4 ^{o}C until analysis. RNA extraction was performed immediately after sample collection using the RNeasy Mini Kit (Qiagen cat# 74104) according to the manufacturer's protocols. Quality of purified RNAs was checked by measuring the absorbance ratio at 260 nm to 280 nm (A260/A280) by using the NanoDrop ND-1000 (Nanodrop Technologies). The RNA integrity and concentration were assessed by using the automated electrophoresis station Agilent TapeStation 4200 (Bio-Rad).

All RNA samples were diluted in RNase/DNase free water (Fisher Scientific cat# BP28191)) at the same concentration and a volume corresponding to 500 ng was added to iScript™ cDNA synthesis kit reagents (Bio-Rad cat# 1708890) for cDNA synthesis, as per the kit instructions.

The reaction mixture was incubated for 5 min at 25 °C, followed by 30 min at 46 °C and 5 min at 95 °C and held at 4 °C. The cDNA samples were then stored at –80 °C.

The qPCR was performed by using the SsoAdvanced™ Universal SYBR Green Supermix (Bio-Rad cat# 1725270). 2 µl of cDNA was used per total of 20 µl reaction mixture as a template. *TFC1* and *UBC6* genes were used as housekeeping genes. See Supplementary Fig. 1 and Table 1 for RNA quality control and primers used. Cycling conditions included a polymerase activation step of 98°C for 2 min and 40 cycles at 98°C for 2 sec and annealing /extension at 60°C for 5 sec followed by melt curve analysis from 65 to 95°C in 0.5°C increments. The sizes of amplicons for each gene were verified on a 2% agarose gel. The ΔCt values were calculated by subtracting the threshold cycle (Ct) of *tagRFP* from the average of the Ct of the two reference genes.

Light-induced degradation and imaging

Yeast cells grown overnight were diluted to an OD_{600} of 1, and the medium was replaced with the induction medium, SG-CAA (0.1 M sodium phosphate, pH 6.0, 6.7 g/L yeast nitrogen base, 5.0 g/L casamino acids, 20.0 g/L galactose) supplemented with tryptophan (0.04 g/L) at 16 ^{o}C on an orbital shaker (250 rpm) for 20 hrs. Cells were kept in the dark during the entire induction period to prevent unwanted degradation. Degradation was activated by delivering blue light (470 nm) at a power density of 0.027 mW/mm^2 (106.02 $\mu mol/m^2s$) using a light-emitting diode (LED, Thorlabs). For imaging tagRFP, green light (530 nm) was delivered at a power density of 0.69 mW/mm^2.

Additional precautions were taken to prevent exposure to light after induction until the experiment was completed. For imaging, cells were placed in 96-wells plates coated with

concanavalin A (2 mg/mL, Sigma Aldrich) to attach the cells to the bottom of the plates. Unbound cells were washed with SG-CAA medium.

The sum of the fluorescence intensity of each microcolony was measured over the experiment to quantify the protein level. To identify regions with microcolonies, 'Otsu dark' auto threshold method in the ImageJ library was used. The mean fluorescence intensity over all microcolonies of all five experiments was defined as the normalization factor. The sum for each microcolony was then normalized to the normalization factor. Additionally, an offset specific to each experiment was used in all experimental datasets so that the first value started at a normalized value of 1. In each experiment, measurements from at least 10 microcolonies were recorded and averaged.

LED intensities were controlled with an Arduino (See **Supplementary Information**) and controlled using the µManager (Edelstein, Tsuchida et al. 2014). The system snaps images from all samples every minute while exposing psd and Δpsd samples to a blue LED controlled via the Java programming language (See **Supplementary Information**). The image processing/analysis was conducted using the ImageJ/µManager libraries (See **Supplementary Information** for more details and the codes are available in GitHub (Mahrou 2021)).

Statistical analysis

To generate the Bode plot, the median phase and amplitude values from each of the five frequencies from ten microcolonies and median of four parameter values estimated for the model were calculated. The median values between the three datasets (Model, tagRFP-psd, and mCherry-psd) were compared using the Nemenyi test. Statistical analyses were performed using real statistics in Excel (Charles Zaiontz, www.real-statistics.com).

Acknowledgements

This work was funded by the University of Connecticut, the Alzheimer's Association (2019-AARG-NTF-640971), and NIH (1R21NS111358-01A1). We thank Bo Reese and Lu Li of Center for Genome Innovation within the Institute for Systems Genomics at the University of Connecticut for their help in the RNA quality assessment and qPCR analysis. The authors declare that they have no conflicts of interest with the contents of this article.

Author Contributions

B.M. designed and performed the experiments, derived the model and analyzed the data. A.P. cloned the psd constructs and conducted the qPCR gene expression analysis. M.H. conducted the statistical analysis. Y.C. and Y.S. supervised the project and assisted with the analysis and the interpretation of data and model. All authors discussed the results and contributed to the manuscript.

References

Antoniou, A. (2016). Digital signal processing, McGraw-Hill. 0071846034

Baaske, J., P. Gonschorek, R. Engesser, A. Dominguez-Monedero, K. Raute, P. Fischbach, K. Muller, E. Cachat, W. W. A. Schamel, S. Minguet, J. A. Davies, J. Timmer, W. Weber and M. D. Zurbriggen (2018). "Dual-controlled optogenetic system for the rapid down-regulation of protein levels in mammalian cells." Sci Rep **8**(1): 15024. 10.1038/s41598-018-32929-7

Banaszynski, L. A., L. C. Chen, L. A. Maynard-Smith, A. G. Ooi and T. J. Wandless (2006). "A rapid, reversible, and tunable method to regulate protein function in living cells using synthetic small molecules." Cell **126**(5): 995-1004. 10.1016/j.cell.2006.07.025

Baracos, V. E. (2000). "Regulation of skeletal-muscle–protein turnover in cancer-associated cachexia." Nutrition **16**(10): 1015-1018.

Batchelor, E., A. Loewer and G. Lahav (2009). "The ups and downs of p53: understanding protein dynamics in single cells." Nature Reviews Cancer **9**(5): 371-377. 10.1038/nrc2604

Bennett, M. R., W. L. Pang, N. A. Ostroff, B. L. Baumgartner, S. Nayak, L. S. Tsimring and J. Hasty (2008). "Metabolic gene regulation in a dynamically changing environment." Nature **454**(7208): 1119.

Bennett, M. R., W. L. Pang, N. A. Ostroff, B. L. Baumgartner, S. Nayak, L. S. Tsimring and J. Hasty (2008). "Metabolic gene regulation in a dynamically changing environment." Nature **454**(7208): 1119-1122. 10.1038/nature07211

Bodvard, K., D. Wrangborg, S. Tapani, K. Logg, P. Sliwa, A. Blomberg, M. Kvarnström and M. Käll (2011). "Continuous light exposure causes cumulative stress that affects the localization oscillation dynamics of the transcription factor Msn2p." Biochimica et Biophysica Acta (BBA) - Molecular Cell Research **1813**(2): 358-366. https://doi.org/10.1016/j.bbamcr.2010.12.004

Bonger, K. M., R. Rakhit, A. Y. Payumo, J. K. Chen and T. J. Wandless (2014). "General method for regulating protein stability with light." ACS Chem Biol **9**(1): 111-115. 10.1021/cb400755b

Ciechanover, A. (2017). "Intracellular protein degradation: from a vague idea thru the lysosome and the ubiquitin-proteasome system and onto human diseases and drug targeting." Best Practice & Research Clinical Haematology **30**(4): 341-355.

Craggs, T. D. (2009). "Green fluorescent protein: structure, folding and chromophore maturation." Chemical Society Reviews **38**(10): 2865-2875.

DeScenzo, R. A. and S. C. Minocha (1993). "Modulation of cellular polyamines in tobacco by transfer and expression of mouse ornithine decarboxylase cDNA." Plant molecular biology **22**(1): 113-127.

Ding, N., S. Zhou and Y. Deng (2021). "Transcription-Factor-based Biosensor Engineering for Applications in Synthetic Biology." ACS Synth Biol **10**(5): 911-922. 10.1021/acssynbio.0c00252

Dohmen, R. J., P. Wu and A. Varshavsky (1994). "Heat-Inducible Degron: a Method for Constructing Temperature-Sensitive Mutants." Science **263**(5151): 1273-1276. 10.1126/science.8122109

Dunlap, J. C. (1999). "Molecular Bases for Circadian Clocks." Cell **96**(2): 271-290. https://doi.org/10.1016/S0092-8674(00)80566-8

Edelstein, A. D., M. A. Tsuchida, N. Amodaj, H. Pinkard, R. D. Vale and N. Stuurman (2014). "Advanced methods of microscope control using μManager software." Journal of Biological Methods **1**(2): e10. 10.14440/jbm.2014.36

Engstrom, M. D. and B. F. Pfleger (2017). "Transcription control engineering and applications in synthetic biology." Synthetic and Systems Biotechnology **2**(3): 176-191. https://doi.org/10.1016/j.synbio.2017.09.003

Evans, T., E. T. Rosenthal, J. Youngblom, D. Distel and T. Hunt (1983). "Cyclin: A protein specified by maternal mRNA in sea urchin eggs that is destroyed at each cleavage division." Cell **33**(2): 389-396. https://doi.org/10.1016/0092-8674(83)90420-8

Faden, F., T. Ramezani, S. Mielke, I. Almudi, K. Nairz, M. S. Froehlich, J. Höckendorff, W. Brandt, W. Hoehenwarter, R. J. Dohmen, A. Schnittger and N. Dissmeyer (2016). "Phenotypes on demand via switchable target protein degradation in multicellular organisms." Nature Communications **7**(1): 12202. 10.1038/ncomms12202

Geva-Zatorsky, N., N. Rosenfeld, S. Itzkovitz, R. Milo, A. Sigal, E. Dekel, T. Yarnitzky, Y. Liron, P. Polak, G. Lahav and U. Alon (2006). "Oscillations and variability in the p53 system." Mol Syst Biol **2**: 2006 0033. 10.1038/msb4100068

Geva□Zatorsky, N., N. Rosenfeld, S. Itzkovitz, R. Milo, A. Sigal, E. Dekel, T. Yarnitzky, Y. Liron, P. Polak and G. Lahav (2006). "Oscillations and variability in the p53 system." Molecular systems biology **2**(1).

Glotzer, M., A. W. Murray and M. W. Kirschner (1991). "Cyclin is degraded by the ubiquitin pathway." Nature **349**(6305): 132-138. 10.1038/349132a0

Goldberg, A. (2007). "Functions of the proteasome: from protein degradation and immune surveillance to cancer therapy." Biochemical Society Transactions **35**(1): 12-17.

Goldbeter, A. (2002). "Computational approaches to cellular rhythms." Nature **420**(6912): 238-245. 10.1038/nature01259

Harton, M. D., W. S. Koh, A. D. Bunker, A. Singh and E. Batchelor (2019). "p53 pulse modulation differentially regulates target gene promoters to regulate cell fate decisions." Molecular Systems Biology **15**(9): e8685. https://doi.org/10.15252/msb.20188685

Hausser, J., A. Mayo, L. Keren and U. Alon (2019). "Central dogma rates and the trade-off between precision and economy in gene expression." Nature Communications **10**(1): 68. 10.1038/s41467-018-07391-8

Herskowitz, I. (1988). "Life cycle of the budding yeast Saccharomyces cerevisiae." Microbiol Rev **52**(4): 536-553. 10.1128/mr.52.4.536-553.1988

Hinkson, I. V. and J. E. Elias (2011). "The dynamic state of protein turnover: It's about time." Trends in cell biology **21**(5): 293-303.

Hirata, H., S. Yoshiura, T. Ohtsuka, Y. Bessho, T. Harada, K. Yoshikawa and R. Kageyama (2002). "Oscillatory Expression of the bHLH Factor Hes1 Regulated by a Negative Feedback Loop." Science **298**(5594): 840-843. doi:10.1126/science.1074560

Hoyt, M. A., M. Zhang and P. Coffino (2003). "Ubiquitin-independent mechanisms of mouse ornithine decarboxylase degradation are conserved between mammalian and fungal cells." J Biol Chem **278**(14): 12135-12143. 10.1074/jbc.M211802200

Huang, D. and E. V. Shusta (2005). "Secretion and surface display of green fluorescent protein using the yeast Saccharomyces cerevisiae." Biotechnol Prog **21**(2): 349-357. 10.1021/bp0497482

Huang, S. and D. E. Ingber (2000). "Shape-dependent control of cell growth, differentiation, and apoptosis: switching between attractors in cell regulatory networks." Experimental cell research **261**(1): 91-103.

Huang, S. and D. E. Ingber (2007). "A non-genetic basis for cancer progression and metastasis: self-organizing attractors in cell regulatory networks." Breast disease **26**(1): 27-54.

Kneppers, A. E., R. C. Langen, H. R. Gosker, L. B. Verdijk, N. C. Lipovec, P. A. Leermakers, M. C. Kelders, C. C. de Theije, D. Omersa and M. Lainscak (2017). "Increased Myogenic and Protein Turnover Signaling in Skeletal Muscle of Chronic Obstructive Pulmonary Disease Patients With Sarcopenia." Journal of the American Medical Directors Association **18**(7): 637. e631-637. e611.

Kume, K., M. J. Zylka, S. Sriram, L. P. Shearman, D. R. Weaver, X. Jin, E. S. Maywood, M. H. Hastings and S. M. Reppert (1999). "mCRY1 and mCRY2 are essential components of the negative limb of the circadian clock feedback loop." Cell **98**(2): 193-205.

Lahav, G. (2004). "The Strength of Indecisiveness: Oscillatory Behavior for Better Cell Fate Determination." Science's STKE **2004**(264): pe55-pe55. 10.1126/stke.2642004pe55

Lahav, G., N. Rosenfeld, A. Sigal, N. Geva-Zatorsky, A. J. Levine, M. B. Elowitz and U. Alon (2004). "Dynamics of the p53-Mdm2 feedback loop in individual cells." Nature Genetics **36**(2): 147-150. 10.1038/ng1293

Lakin, N. D. and S. P. Jackson (1999). "Regulation of p53 in response to DNA damage." Oncogene **18**(53): 7644-7655. 10.1038/sj.onc.1203015

Lev Bar-Or, R., R. Maya, L. A. Segel, U. Alon, A. J. Levine and M. Oren (2000). "Generation of oscillations by the p53-Mdm2 feedback loop: a theoretical and experimental study." Proc Natl Acad Sci U S A **97**(21): 11250-11255. 10.1073/pnas.210171597

Ljung, L. (1998). System identification. Signal analysis and prediction. Boston, MA, Springer**:** 163-173. 10.1007/978-1-4612-1768-8_11

Luh, L. M., U. Scheib, K. Juenemann, L. Wortmann, M. Brands and P. M. Cromm (2020). "Prey for the Proteasome: Targeted Protein Degradation—A Medicinal Chemist's Perspective." Angewandte Chemie International Edition **59**(36): 15448-15466. https://doi.org/10.1002/anie.202004310

Mahrou, B. (2021). "Degradation driven protein turnover." from https://github.com/Bam12006/The-low-pass-filtering-effect-of-degradation-driven-protein-turnover.

Merzlyak, E. M., J. Goedhart, D. Shcherbo, M. E. Bulina, A. S. Shcheglov, A. F. Fradkov, A. Gaintzeva, K. A. Lukyanov, S. Lukyanov and T. W. Gadella (2007). "Bright monomeric red fluorescent protein with an extended fluorescence lifetime." Nature methods **4**(7): 555.

Mizushima, N. and D. J. Klionsky (2007). "Protein turnover via autophagy: implications for metabolism." Annu. Rev. Nutr. **27**: 19-40.

Monk, N. A. (2003). "Oscillatory expression of Hes1, p53, and NF-kappaB driven by transcriptional time delays." Curr Biol **13**(16): 1409-1413. 10.1016/s0960-9822(03)00494-9

Murakami, Y., S. Matsufuji, T. Kameji, S. Hayashi, K. Igarashi, T. Tamura, K. Tanaka and A. Ichihara (1992). "Ornithine decarboxylase is degraded by the 26S proteasome without ubiquitination." Nature **360**(6404): 597-599. 10.1038/360597a0

Natsume, T. and M. T. Kanemaki (2017). "Conditional Degrons for Controlling Protein Expression at the Protein Level." Annu Rev Genet **51**: 83-102. 10.1146/annurev-genet-120116-024656

Nishimura, K., T. Fukagawa, H. Takisawa, T. Kakimoto and M. Kanemaki (2009). "An auxin-based degron system for the rapid depletion of proteins in nonplant cells." Nat Methods **6**(12): 917-922. 10.1038/nmeth.1401

Novák, B. and J. J. Tyson (2008). "Design principles of biochemical oscillators." Nature reviews Molecular cell biology **9**(12): 981-991.

Piette, J., H. Neel and V. Maréchal (1997). "Mdm2: keeping p53 under control." Oncogene **15**(9): 1001-1010. 10.1038/sj.onc.1201432

Porter, Joshua R., Brian E. Fisher and E. Batchelor (2016). "p53 Pulses Diversify Target Gene Expression Dynamics in an mRNA Half-Life-Dependent Manner and Delineate Co-regulated Target Gene Subnetworks." Cell Systems **2**(4): 272-282. https://doi.org/10.1016/j.cels.2016.03.006

Pourquié, O. (2003). "The Segmentation Clock: Converting Embryonic Time into Spatial Pattern." Science **301**(5631): 328-330. doi:10.1126/science.1085887

Pratt, J. M., J. Petty, I. Riba-Garcia, D. H. Robertson, S. J. Gaskell, S. G. Oliver and R. J. Beynon (2002). "Dynamics of protein turnover, a missing dimension in proteomics." Molecular & Cellular Proteomics **1**(8): 579-591.

Purcell, O., N. J. Savery, C. S. Grierson and M. di Bernardo (2010). "A comparative analysis of synthetic genetic oscillators." Journal of The Royal Society Interface **7**(52): 1503-1524. 10.1098/rsif.2010.0183

Renicke, C., D. Schuster, S. Usherenko, L.-O. Essen and C. Taxis (2013). "A LOV2 domain-based optogenetic tool to control protein degradation and cellular function." Chemistry & biology **20**(4): 619-626.

Renicke, C., D. Schuster, S. Usherenko, L. O. Essen and C. Taxis (2013). "A LOV2 domain-based optogenetic tool to control protein degradation and cellular function." Chem Biol **20**(4): 619-626. 10.1016/j.chembiol.2013.03.005

Reppert, S. M. and D. R. Weaver (2001). "Molecular Analysis of Mammalian Circadian Rhythms." Annual Review of Physiology **63**(1): 647-676. 10.1146/annurev.physiol.63.1.647

Robertson, J. B., C. R. Davis and C. H. Johnson (2013). "Visible light alters yeast metabolic rhythms by inhibiting respiration." Proc Natl Acad Sci U S A **110**(52): 21130-21135. 10.1073/pnas.1313369110

Sayed, A. H. (2011). Adaptive filters, John Wiley & Sons. 1118210840

Shin, Y.-J. (2016). "Digital Signal Processing and Control for the Study of Gene Networks." Scientific reports **6**: 24733.

Stankunas, K., J. H. Bayle, J. E. Gestwicki, Y.-M. Lin, T. J. Wandless and G. R. Crabtree (2003). "Conditional Protein Alleles Using Knockin Mice and a Chemical Inducer of Dimerization." Molecular Cell **12**(6): 1615-1624. https://doi.org/10.1016/S1097-2765(03)00491-X

Strickland, D., X. Yao, G. Gawlak, M. K. Rosen, K. H. Gardner and T. R. Sosnick (2010). "Rationally improving LOV domain-based photoswitches." Nat Methods **7**(8): 623-626. 10.1038/nmeth.1473

Subach, F. V. and V. V. Verkhusha (2012). "Chromophore transformations in red fluorescent proteins." Chem Rev **112**(7): 4308-4327. 10.1021/cr2001965

Sun, W., W. Zhang, C. Zhang, M. Mao, Y. Zhao, X. Chen and Y. Yang (2017). "Light-induced protein degradation in human-derived cells." Biochem Biophys Res Commun **487**(2): 241-246. 10.1016/j.bbrc.2017.04.041

Takeuchi, J., H. Chen, Martin A. Hoyt and P. Coffino (2008). "Structural elements of the ubiquitin-independent proteasome degron of ornithine decarboxylase." Biochemical Journal **410**(2): 401-407. 10.1042/BJ20071239

Talia, S. D., J. M. Skotheim, J. M. Bean, E. D. Siggia and F. R. Cross (2007). "The effects of molecular noise and size control on variability in the budding yeast cell cycle." Nature **448**(7156): 947-951. 10.1038/nature06072

Taxis, C., G. Stier, R. Spadaccini and M. Knop (2009). "Efficient protein depletion by genetically controlled deprotection of a dormant N-degron." Molecular Systems Biology **5**(1): 267. https://doi.org/10.1038/msb.2009.25

Teste, M.-A., M. Duquenne, J. M. François and J.-L. Parrou (2009). "Validation of reference genes for quantitative expression analysis by real-time RT-PCR in Saccharomyces cerevisiae." BMC molecular biology **10**(1): 99.

Tiana, G., S. Krishna, S. Pigolotti, M. H. Jensen and K. Sneppen (2007). "Oscillations and temporal signalling in cells." Phys Biol **4**(2): R1-17. 10.1088/1478-3975/4/2/r01

Tigges, M. and M. Fussenegger (2009). "Recent advances in mammalian synthetic biology-design of synthetic transgene control networks." Curr Opin Biotechnol **20**(4): 449-460. 10.1016/j.copbio.2009.07.009

Varshavsky, A. (2008). "Discovery of cellular regulation by protein degradation." Journal of Biological Chemistry **283**(50): 34469-34489.

Varshavsky, A. (2019). "N-degron and C-degron pathways of protein degradation." Proceedings of the National Academy of Sciences **116**(2): 358-366. 10.1073/pnas.1816596116

Vilar, J. M., H. Y. Kueh, N. Barkai and S. Leibler (2002). "Mechanisms of noise-resistance in genetic oscillators." Proc Natl Acad Sci U S A **99**(9): 5988-5992. 10.1073/pnas.092133899

Vogel, C. and E. M. Marcotte (2012). "Insights into the regulation of protein abundance from proteomic and transcriptomic analyses." Nature Reviews Genetics **13**(4): 227.

Wachter, R. M. (2007). "Chromogenic cross-link formation in green fluorescent protein." Accounts of chemical research **40**(2): 120-127.

Wei, C.-L., Q. Wu, V. B. Vega, K. P. Chiu, P. Ng, T. Zhang, A. Shahab, H. C. Yong, Y. Fu and Z. Weng (2006). "A global map of p53 transcription-factor binding sites in the human genome." Cell **124**(1): 207-219.

Woods, M. L., M. Leon, R. Perez-Carrasco and C. P. Barnes (2016). "A Statistical Approach Reveals Designs for the Most Robust Stochastic Gene Oscillators." ACS Synthetic Biology **5**(6): 459-470. 10.1021/acssynbio.5b00179